Research Article J. Electrochem. Sci. Technol., 2017, 8(1), 25-34

Journal of Electrochemical Science and Technology
jecst.org

Concurrent Electrocatalysis and Sensing of Hydrazine and Sulfite and Nitrite Ions using Electrodeposited Gold Nanostructure-Modified Electrode

Yeji Seo, Shanmugam Manivannan*, Inhak Kang, Woo-Seung Shin, and Kyuwon Kim*
Electrochemistry Laboratory for Sensors & Energy (ELSE), Department of Chemistry, Incheon National University, Incheon 406-772, Republic of Korea.

ABSTRACT

Concurrent electrocatalysis and sensing of hydrazine, sulfite ions, and nitrite ions in a mixture were studied using electrodes modified by electrodeposited Au nanostructures (NSs). The β-cyclodextrin–mixed silicate sol-gel composite was drop-casted on the electrode surface and nucleation guided by β-cyclodextrin occurred, followed by the electrodeposition of Au NSs. The additive, β-cyclodextrin, played an evident role as a structure-directing agent; thus, small raspberry-like Au NSs were obtained. The modified electrodes were characterized by surface characterization techniques and electrochemical methods. The Au NSs-modified electrodes effciently electrocatalyzed the oxidation of toxic molecules such as hydrazine and sulfite and nitrite ions even in the absence of any other electron transfer mediator or enzyme immobilization. Well-resolved oxidation peaks along with decreased overpotentials were noticed during the electrooxidation process. The fabricated Au nanostructured electrode clearly distinguished the electrooxidation peaks of each of the three analytes from their mixture.

Keywords : Electrocatalysis, Electrochemical sensor, Gold nanostructures, Hydrazine, Nitrite, Sulfite

Received : 5 December 2016, Accepted : 2 January 2017

1. Introduction

The impact of the environmental accumulation and contamination of hydrazine (N_2H_4) and sulfite (SO_3^{2-}) and nitrite (NO_2^-) ions on the human health and ecosystem is a major concern [1-4]. Concurrent monitoring of the variations in the concentrations of N_2H_4, SO_3^{2-}, and NO_2^- is essential for understanding their biogeochemical processes in aquatic environments and to develop better strategies for managing the water quality, wastewater treatment, and food industry. Hydrazine is widely used as a starting material in the production of some insecticides, herbicides, pesticides, dyestuffs, and explosives, as well as in the preparation of several pharmaceutical derivatives [5]. The N_2H_4 is also an ideal fuel for the direct fuel cell system because its fuel electrooxidation process does not suffer from any poisoning effects [6-9]. Compounds containing SO_3^{2-} ions are used as preservatives in view of their antioxidant properties and as inhibitors of enzymatic and microbial activities in beverages, food, and pharmaceutical products [10]. The NO_2^- ion is a typical inorganic pollutant and its sources include wastes from fertilizer and preservative industries and adulterants in food [11-14]. Therefore, it is important and desirable to design and develop a catalyst for the concurrent detection and determination of N_2H_4, SO_3^{2-}, and NO_2^- present in food, water, biological fluids, etc. Electrochemical techniques have been found to be the most promising methods for the determination of N_2H_4, SO_3^{2-}, and NO_2^- [12]. Electrochemical oxidation of these analytes at a bare electrode is normally accompanied with a high overpotential, which represents a slug-

*E-mail address: kyuwon_kim@inu.ac.kr, smanivannan1982@yahoo.com
DOI: https://doi.org/10.5229/JECST.2017.8.1.25

gish electron transfer process. Hence, distinguishing each analyte's redox behavior is not possible at the bare electrode. The facile modification of the electrode surface would reduce the overpotential and increase the catalytic current for such analytes [15-17]. Such surface-modified electrodes enhance the rate of electron transfer by reducing the overpotential associated with the reaction and could distinguish the redox behavior of each of the analyte.

Au nanostructures (NSs) have attracted much attention as an electrocatalyst that exhibits higher catalytic activity toward various analytes [14,18,19]. The electrocatalytic property of Au nanoparticles (NPs) mainly depends on their preparation methods [19,20]. Previously, Maduraiveeran et al. [15] reported the concurrent sensing of N_2H_4, SO_3^{2-}, and NO_2^- with a large decrease in the overpotentials using a colloidal Au NPs-modified electrode. In the present work, the concurrent electrocatalytic oxidation and sensing were studied using a mixture of N_2H_4, SO_3^{2-}, and NO_2^- electrodeposited at the Au NS-modified electrode. β-Cyclodextrin (CD) mixed with amine-functionalized silicate sol–gel matrix (SSG) composite was used to modify the glassy carbon (GC) electrode surface prior to electrodeposition. For Au deposition, CD was used as an additive, and it acted as a structure-directing agent. The results were compared with those of the Au NSs fabricated in the absence of CD.

2. Experimental Section

2. 1 Materials and methods

Gold(III) chloride ($HAuCl_4$), β-cyclodextrin, *N'*-[3-(trimethoxysilyl) propyl] diethylenetriamine (silane monomer used to prepare SSG), and hexaammineruthenium(III) chloride ($Ru(NH_3)_6Cl_3$) were obtained from Sigma-Aldrich. Hydrazine hydrate, sodium sulfite, and sodium nitrite were purchased from Merck. All the glassware was thoroughly cleaned with aqua regia (HNO_3/HCl (1:3) v/v) (caution: *aqua regia is a powerful oxidizing agent and it should be handled with extreme care*) and rinsed extensively with distilled water before use. The scanning electron microscopy (SEM) images were obtained for the electrodeposited films on an indium tin oxide (ITO) substrate using a JEOL JSM-7800F. We have used the ITO electrodes only for SEM measurements and the GC electrode for electrochemical studies. The cyclic voltammograms (CVs) and square wave voltammograms (SWVs) of the modified electrodes were recorded using Ivium Technologies' electrochemical workstation. The electrochemical experiments were performed using a single-compartment three-electrode cell. The GC electrode (with a geometric area of 0.07 cm^2) was used as the working electrode and a platinum wire as the counter electrode. The reference electrode was Ag/AgCl (in 3M NaCl). The electrolyte solution was deaerated by purging nitrogen gas for 30 min prior to each experiment.

2.2 Preparation of SSG-CD composite

A homogeneous SSG-CD composite was prepared [19] by the addition of 10 μL of 1 M silane monomer to 10 mL of 7 mM aqueous CD solution under vigorous stirring and the stirring was continued for another 60 min.

2.3 Electrode fabrication

The Au NSs-modified electrodes were prepared using a previously reported procedure [21]. Briefly, a known amount (5 μL) of SSG or SSG-CD composite was drop-casted on the GC electrode and allowed to dry at 37°C for 1 h. The Au NSs were electrodeposited at the modified electrode by applying a potential of -0.2 V (Ag/AgCl) for 300 s using an electrolyte solution containing 3 mM $HAuCl_4$ and 0.5 M H_2SO_4. The prepared modified electrodes are represented as GC/Au, GC/SSG-Au, and GC/SSG-CD-Au. For the SEM measurements, ITO electrodes (1 × 2 cm) were used instead of the GC electrode. The drop-casted composite volume was 50 μL. The remaining experimental parameters were the same as in the previously reported procedure.

2.4 Concurrent electrocatalysis and sensing

The experiments were carried out using a 100 μM of each analyte (N_2H_4, SO_3^{2-}, and NO_2^-). During the measurements, a solution of N_2H_4, SO_3^{2-}, and NO_2^- was added to a 0.1 M PBS buffer electrolyte solution (pH = 7.2).

3. Results and Discussion

3.1 Surface and electrochemical characterization of the modified electrodes

To understand the morphology of the different

modified electrodes, the SEM analysis was performed and the images are shown in Fig. 1 and 2. The ITO/SSG-CD electrode without any electrodeposited Au NSs showed a clear image of the SSG film (Fig. 1A). The Au NSs at the ITO/SSG-Au electrode (Fig. 1B) showed randomly inter-connected structures. At the ITO/Au electrode, the Au NSs resembled flower-like structures (Fig. 1C). However, in the presence of CD in the modified surface of the electrode, the Au NSs were deposited in a different manner at the ITO/SSG-CD electrode (Fig. 1D). The electrodeposited

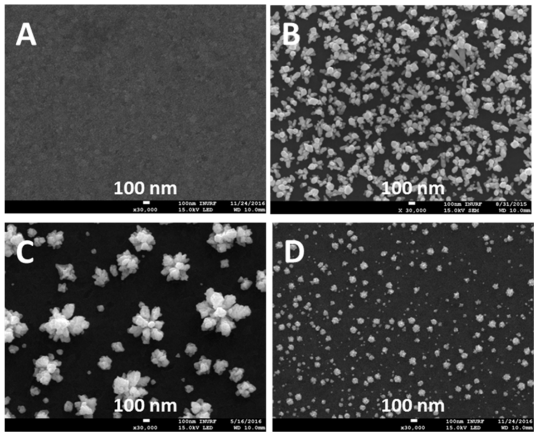

Fig. 1. SEM images of (A) ITO/SSG-CD, (B) ITO/SSG-Au, (C) ITO/Au, and (D) ITO/SSG-CD-Au electrode surfaces.

NSs were smaller than those at the other two electrodes and were not inter-connected with each other. The growth of such small Au NSs at the ITO/SSG-CD electrode can be envisaged, as the nucleation of atomic gold in the presence of CD forms Au atomic clusters. The SSG-CD composite at the electrode surface stabilizes the Au atomic clusters, aided by the hydrogen bonding interaction between the secondary -OH groups of CD. The Au nucleation centers favor bonding with the other Au nucleation centers, leading to the formation of such small Au NSs [21]. Furthermore, higher magnification images (Fig. 2A-D) revealed the size and shape of the deposited NSs. As Fig. 2C shows, the Au NSs resembled raspberry-like structures, as reported previously [21]. SEM-energy dispersive X-ray (EDX) analysis (Fig. 2E and F) clearly revealed the active presence of CD on the electrode surface and that the NSs were composed of elemental Au.

We have used the ITO electrodes only for SEM measurements because the conventional GC electrodes cannot be used for SEM. The electrochemical studies were carried out using the GC electrode. Besides, switching between the ITO and GC substrates would have a negligible impact on the results of this study. Furthermore, the modified surface film (SSG-CD) contributed majorly to the nucleation and growth of the NSs. The Au NSs-deposited electrodes were electrochemically characterized by recording

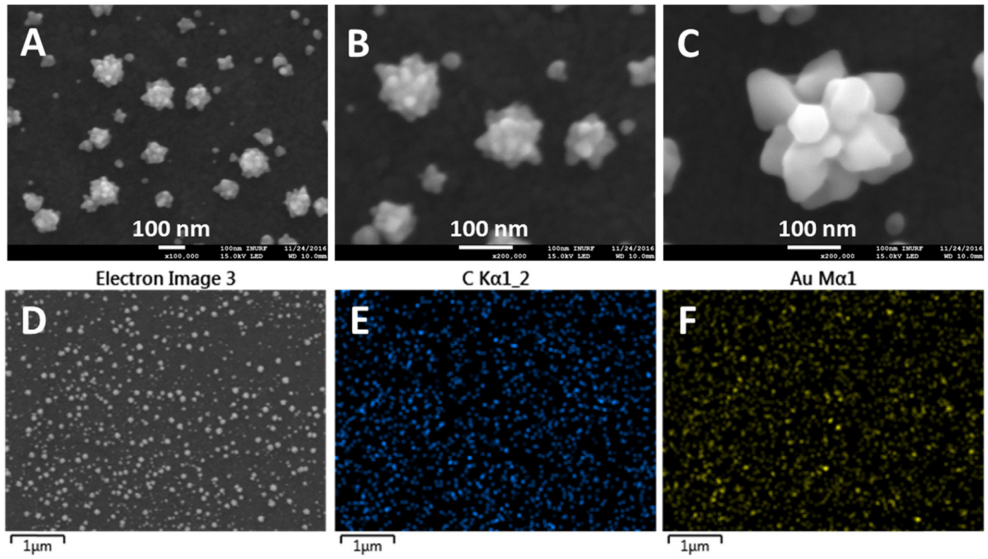

Fig. 2. (A-D) SEM images and (E and F) SEM-EDX analysis images of the ITO/SSG-CD-Au electrode surface.

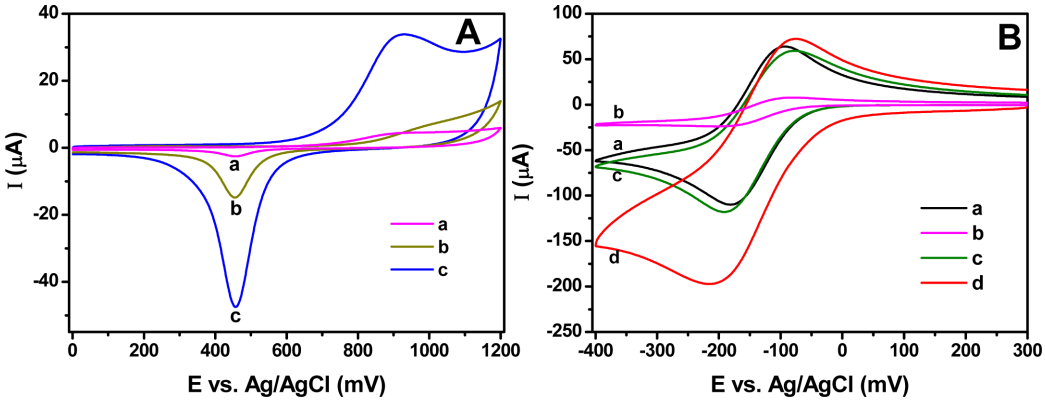

Fig. 3. (A) Cyclic voltammograms recorded at (a) GC/SSG-Au, (b) GC/Au, and (c) GC/SSG-CD-Au electrodes in deaerated 0.1 M PBS buffer (pH = 7.2) at a scan rate of 50 mV/s. (B) Cyclic voltammograms recorded for 3 mM of $[Ru(NH_3)_6]^{3+}$ at (a) bare GC, (b) GC/SSG, (c) GC/SSG-CD, and (d) GC/SSG-CD-Au electrodes in deaerated 0.1 M PBS buffer (pH = 7.2) and 0.1 M KCl at a scan rate of 50 mV/s.

the CVs in the deaerated PBS buffer (pH = 7.2) (Fig. 3A). The oxidation peaks observed around 0.93 V (Fig. 3A(a-c)) were ascribed to the formation of Au oxide and the corresponding reduction peaks were observed around 0.46 V (Fig. 3A(a-c)) because of the reduction of Au oxides [21,22]. Among the different modified electrodes, an increase in the anodic and cathodic peak currents was noticed for the GC/SSG-CD-Au electrode because the highly active Au surface rabidly formed the Au oxide layer at this particular electrode surface. Since the formation of the Au surface oxide and its subsequent reduction are pH dependent [15], a negative shift in the oxidation and reduction peaks (0.927 and 0.455 V, respectively) was observed in the PBS buffer (pH = 7.2), compared to those in an acidic medium (0.5 M H_2SO_4) for all the Au NSs-modified electrodes [23].

The redox behavior of $[Ru(NH_3)_6]^{3+}$ is a valuable tool for testing the kinetic barrier of the interface because the electron transfer between the species in solution and the electrode must occur by electron tunneling through the defects or pinholes in the modified electrode [24]. Fig. 3B(a-d) shows the cyclic voltammetric responses of the bare GC, GC/SSG, GC/SSG-CD, and GC/SSG-CD-Au electrodes, respectively, toward the $[Ru(NH_3)_6]^{3+}$ redox marker. As expected, $[Ru(NH_3)_6]^{3+}$ exhibited reversible behavior at the bare GC electrode (Fig. 3B(a)) with a peak-to-peak separation (ΔEp) of 83 mV at a scan rate of 50 mV/s in 0.1 M PBS and 0.1 M KCl. The GC/SSG electrode (Fig. 3B(b)) showed a quasi-reversible voltammetric response with a very low peak current and a peak-to-peak separation of 123 mV. The higher peak potential difference (ΔEp) observed at the GC/SSG electrode compared to the bare GC electrode is a measure of the kinetic hindrance/repulsion exerted by SSG toward the electron-transfer process at the electrode surface for the $[Ru(NH_3)_6]^{3+}$ ions. This observation (Fig. 3B(b)) revealed that a small amount of the $[Ru(NH_3)_6]^{3+}$ ions might diffuse through the pinholes present in SSG. Such pinholes formations are expected during the swelling of SSG. The GC/SSG-CD electrode (Fig. 3B(c)) showed a quasi-reversible voltammetric response with a peak current higher than that of the GC/SSG electrode (Fig. 3B(b)). Furthermore, the response was almost equal to that observed at the bare GC (Fig. 3B(a)) and the peak-to-peak separation was 116 mV. Since the CD molecule is electrochemically inert, one cannot expect any electrocatalytic effect of CD on the $[Ru(NH_3)_6]^{3+}$ ions. The basic pH (i.e., 9.84) [21] of the SSG-CD composite caused the deprotonation of the -OH groups in the CD molecules, thereby making the electrode negatively charged and showing permselective behavior toward the positively charged $[Ru(NH_3)_6]^{3+}$ ions. Each peak in the CV corresponds to a particular electroactive species in the test solution, and the height of the peak is proportional to the concentration of the analyte. In this case, the deprotonation of -OH groups at the GC/SSG-CD electrode made it negatively charged, and hence, the electrode exhibited permselective behavior toward the posi-

tively charged $[Ru(NH_3)_6]^{3+}$ ions. Due to this preconcentration effect, the $[Ru(NH_3)_6]^{3+}$ ions both from the solution and those adsorbed on the electrode collectively get reduced by Au, leading to an increased reduction current. During the reverse cycle, such preconcentrating effect of the corresponding species was not observed. Hence, there is asymmetry in the behavior of the redox peaks. The GC/SSG-CD-Au electrode (Fig. 3B(d)) also showed a quasi-reversible voltammetric response with a peak current higher than that of the other modified electrodes (Fig. 3B(a-c)), and the peak-to-peak separation was measured to be 133 mV. This observation clearly revealed that the GC/SSG-CD-Au electrode acts as a new electrode with increased electrode area [21,25] and that the Au NSs at the electrode achieve good electrical communication with the underlying electrode surface. It is evident from the higher peak current that the presence of Au NSs at the SSG-CD film shows a marked influence on the barrier property of the GC/SSG-modified electrode.

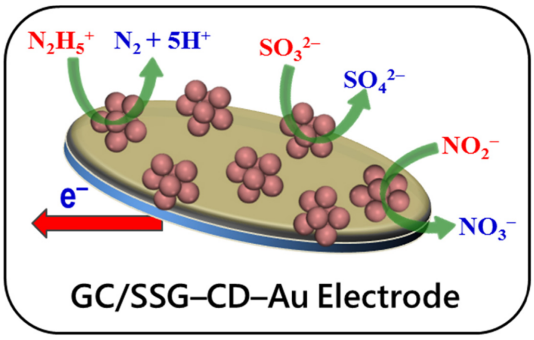

Fig. 4. Schematic representation of simultaneous electrooxidation of N_2H_4, SO_3^{2-}, and NO_2^- at the Au NRBs-modified electrode (GC/SSG-CD-Au).

3.2 Concurrent electrooxidation of N_2H_4, SO_3^{2-}, and NO_2^- mixture

In order to evaluate the electrocatalytic ability of the different fabricated Au NSs, the electrooxidation of N_2H_4, SO_3^{2-}, and NO_2^- was studied both individually and concurrently by cyclic voltammetry. The concurrent electrooxidation of the target analytes at the GC/SSG-CD-Au electrode is schematically represented in Fig. 4. Fig. 5(A-C) displays the CVs

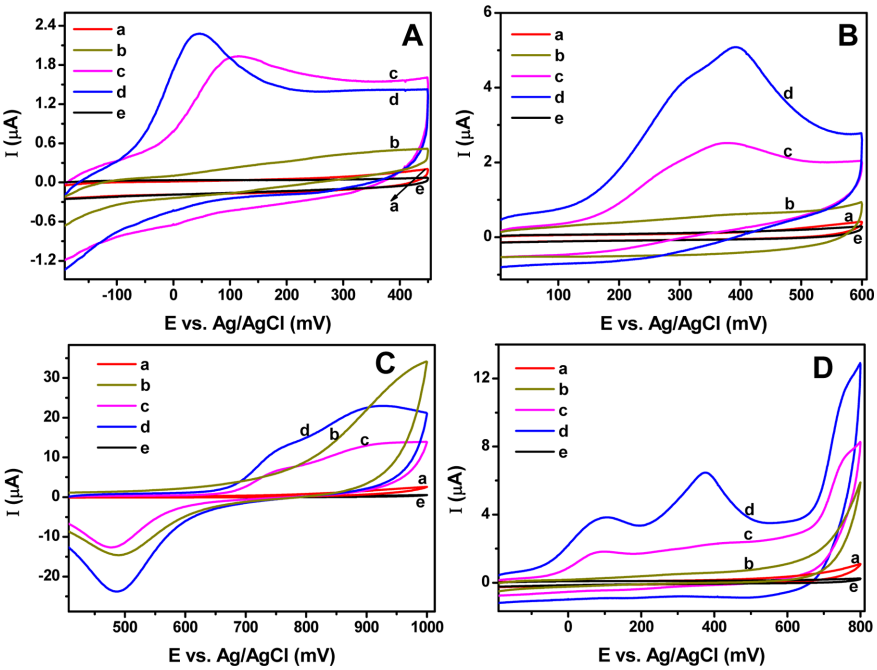

Fig. 5. Cyclic voltammograms obtained for the electrooxidation of 100 μM each of (A) N_2H_4, (B) SO_3^{2-}, and (C) NO_2^-. (D) Cyclic voltammograms showing concurrent electrooxidation of a mixture of 100 μM each of N_2H_4, SO_3^{2-} and NO_2^- at the (a) bare GC, (b) GC/Au, (c) GC/SSG-Au, and (d) GC/SSG-CD-Au electrodes and (e) without any analyte in 0.1 M PBS buffer (pH = 7.2) at a scan rate of 50 mV/s.

observed for the electrooxidation of 100 μM each of N_2H_4, SO_3^{2-}, and NO_2^-, respectively, at the different modified electrodes. Fig. 5D represents the concurrent electrooxidation of a mixture of N_2H_4, SO_3^{2-}, and NO_2^- (100 μM each) at the different modified electrodes. It was observed that N_2H_4, SO_3^{2-}, and NO_2^- cannot be electrooxidized at the bare GC electrode (Fig. 5(A-D)(a)) within the chosen potential window. The GC/Au electrode exhibited poor electrooxidation behavior for all the three analytes and the mixture (Fig. 5(A-D)(b)). Under the same experimental conditions, the GC/SSG-Au electrode exhibited improved catalytic activity toward all the analytes (Fig. 5(A-D)(c)). However, the GC/SSG-CD-Au electrode demonstrated an increase in the anodic peak currents (Fig. 5(A-D)(d)) and also successfully resolved the electrooxidation peaks of all the three analytes (Fig. 5D(d)). In the absence of the analytes, electrochemical responses were not observed at the GC/SSG-CD-Au electrode (Fig. 5(A-D)(e)). The CVs obtained at the GC/SSG-CD-Au electrode demonstrated a decreased overpotential (E_{pa}) and an enhanced peak current (I_{pa}). Furthermore, the cathodic peak observed around 0.5 V in Fig. 5C could be attributed to the reduction of the Au surface oxides [21].

The experimental results showed well-resolved oxidation peaks for the mixture of 100 μM each of N_2H_4, SO_3^{2-}, and NO_2^- at the GC/SSG-CD-Au electrode (Fig. 5D(d)) in 0.1 M PBS at 0.100, 0.375, and 0.757 V, respectively, compared to those at the bare GC, GC/Au and GC/SSG-Au electrodes, which were in good agreement with the previous report [15]. The electrochemical responses observed for the mixture were irreversible and no cathodic current was observed during the reverse cycle (Fig. 5D(d)). The faster electron transfer lead to well-resolved peaks and a considerable increase in the peak currents at the GC/SSG-CD-Au electrode. Hence, the N_2H_4, SO_3^{2-}, and NO_2^- species in a mixture can be monitored effectively and simultaneously at the GC/SSG-CD-Au electrode, without any redox mediator or enzyme immobilization.

3.3 Concurrent electrochemical sensing of N_2H_4, SO_3^{2-}, and NO_2^- in a mixture

Individual SWVs of N_2H_4, SO_3^{2-}, and NO_2^- were studied (Figs. 6, 7, and 8) at the different modified

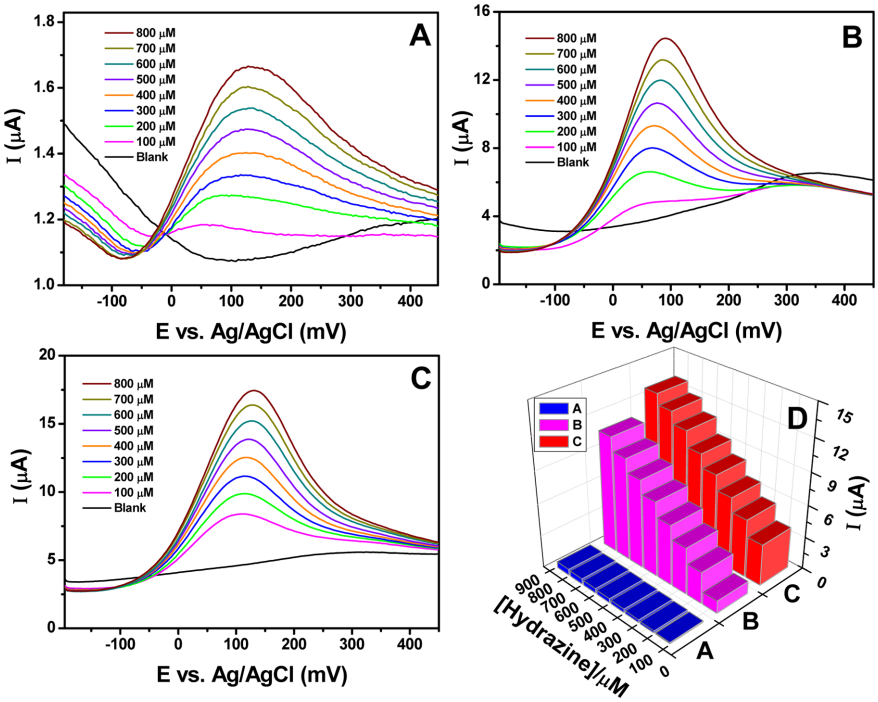

Fig. 6. Square wave voltammograms obtained for each addition of 100 μM N_2H_4 at the (A) GC/SSG-Au, (B) GC/Au, and (C) GC/SSG-CD-Au electrodes in 0.1 M PBS buffer (pH = 7.2). D: Corresponding calibration plot.

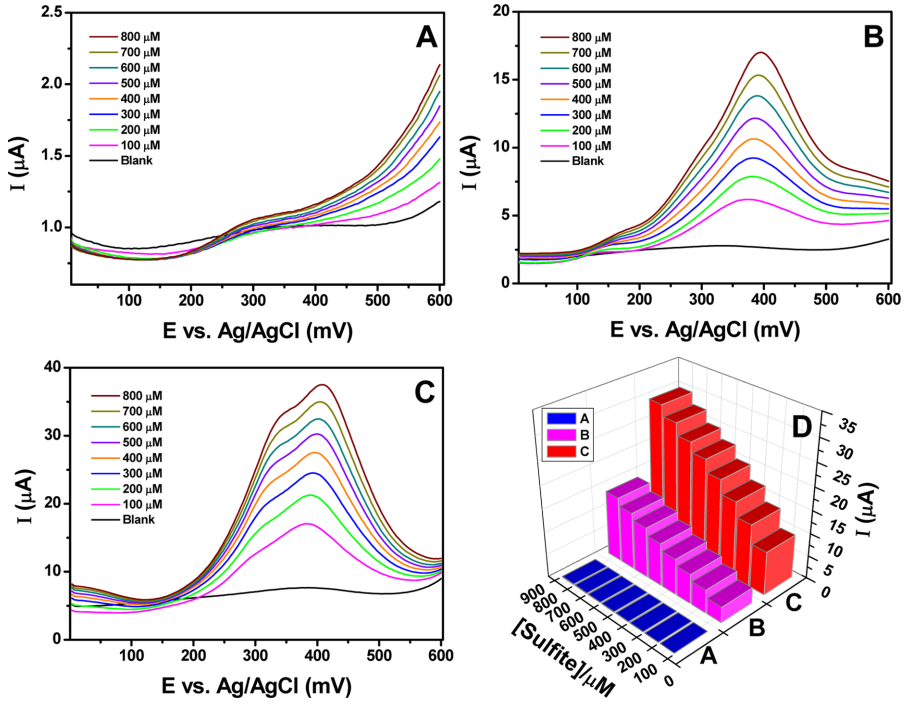

Fig. 7. Square wave voltammograms obtained for each addition of 100 μM SO_3^{2-} at (A) GC/SSG-Au, (B) GC/Au, and (C) GC/SSG-CD-Au electrodes in 0.1 M PBS buffer (pH = 7.2). D: Corresponding calibration plot.

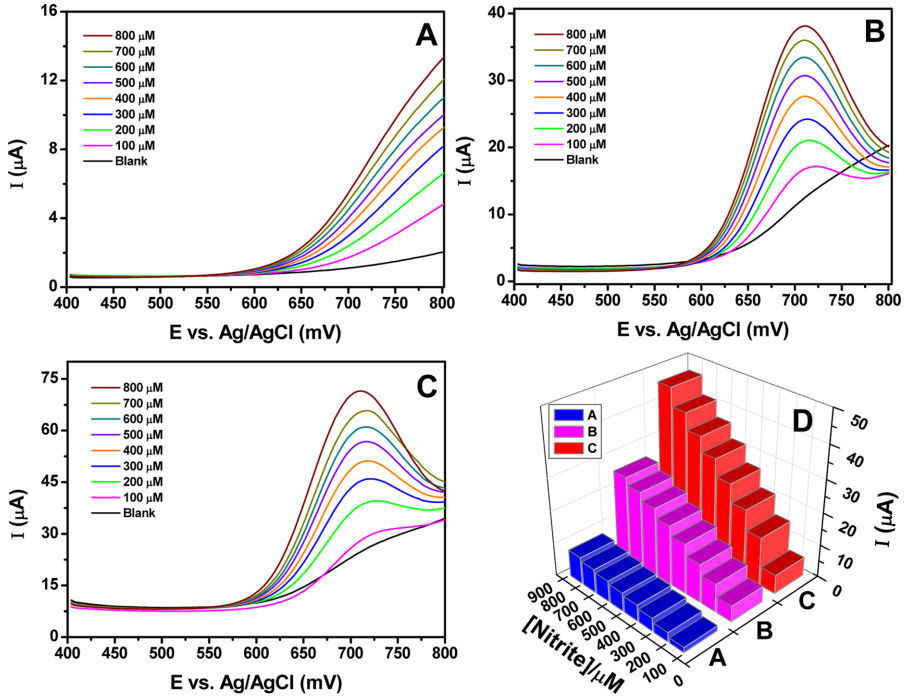

Fig. 8. Square wave voltammograms obtained for each addition of 100 μM NO_2^- at (A) GC/SSG-Au, (B) GC/Au, and (C) GC/SSG-CD-Au electrodes in 0.1 M PBS buffer (pH = 7.2). D: Corresponding calibration plot.

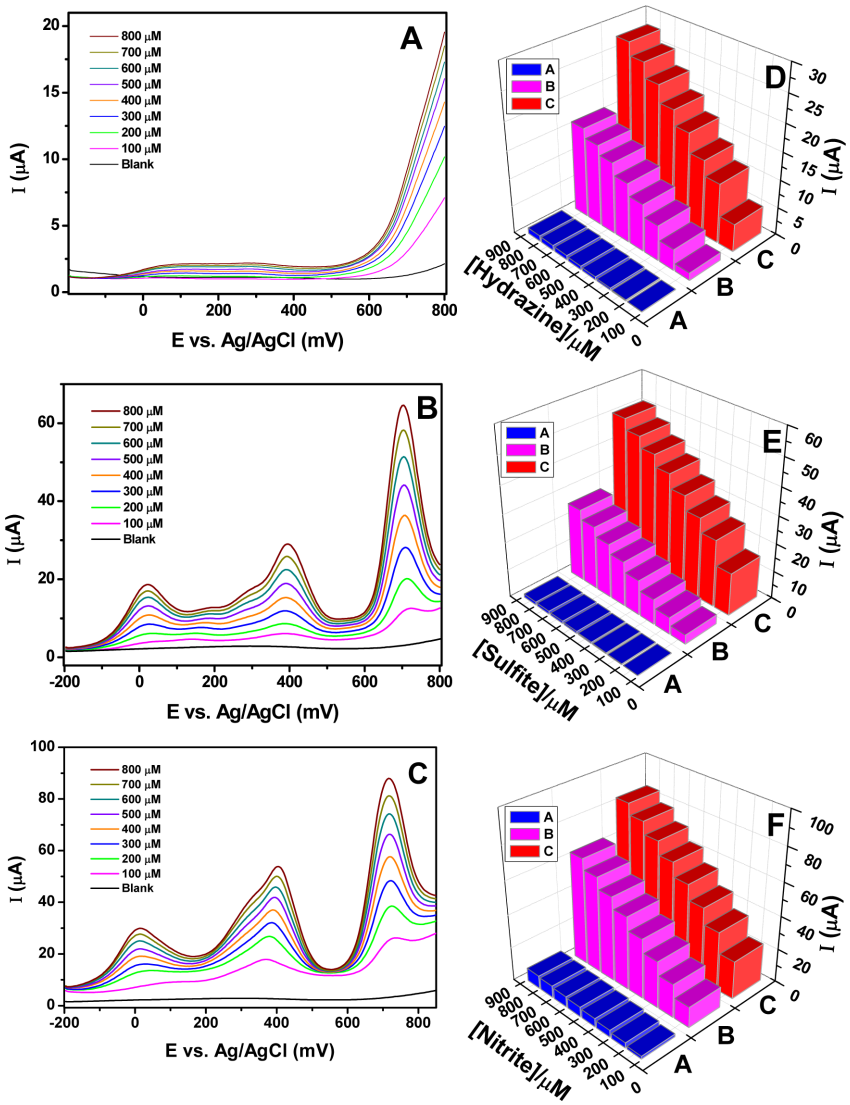

Fig. 9. Simultaneous square wave voltammograms obtained for each addition of 100 μM N_2H_4, SO_3^{2-}, and NO_2^- to their mixture at the (A) GC/SSG-Au, (B) GC/Au, and (C) GC/SSG-CD-Au electrodes in 0.1 M PBS buffer (pH = 7.2). D-F: Corresponding calibration plot.

electrodes. Similar to the electrooxidation behavior, a better electrochemical sensing ability was observed at the GC/SSG-CD-Au electrode for the mixture of analytes with linearly increasing peak currents corresponding to the increasing concentrations of analytes. Furthermore, the sensitivities of the modified electrode for the oxidation of N_2H_4, SO_3^{2-}, and NO_2^- were found to be 0.012, 0.028, and 0.055 μA/μM, respectively, and the respective correlation coefficients (n = 8) were found to be 0.9970, 0.9890, and 0.9880 (Fig. 10A). The sensitivities of the GC/SSG-CD-Au electrode for NO_2^- and SO_3^{2-} were 4.6 and 2.3 times higher than that for N_2H_4, respectively.

Fig. 9(A-C) illustrates the SWVs observed for the mixture of N_2H_4, SO_3^{2-}, and NO_2^- at the GC/SSG-Au (A), GC/Au (B), and GC/SSG-CD-Au (C) electrodes with the successive addition of 100 μM of the analytes and their corresponding calibration plots (Fig. 9(D-F)). Among the three different electrodes, the GC/SSG-Au electrode (Fig. 9A) failed to resolve and

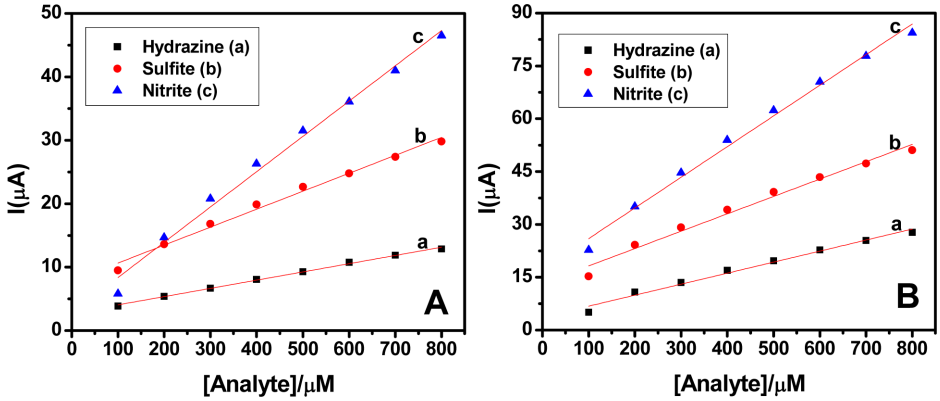

Fig. 10. Calibration plots obtained for the (**A**) individual and (**B**) simultaneous square wave voltammograms obtained for (**a**) N_2H_4, (**b**) SO_3^{2-}, and (**c**) NO_2^- at the GC/SSG-CD-Au electrode in 0.1 M PBS buffer (pH = 7.2).

sense the analytes, whereas the GC/Au (Fig. 9B) and GC/SSG-CD-Au (Fig. 9C) electrodes showed well-resolved oxidation peaks. The peak currents observed at the GC/SSG-CD-Au electrode for the mixture of analytes increased linearly with increasing analyte concentrations (Fig. 10B). The sensitivities of the electrode for N_2H_4, SO_3^{2-}, and NO_2^- were found to be 0.0312, 0.0493, and 0.0870 μA/μM, respectively, and the corresponding correlation coefficients (n = 8) were found to be 0.9830, 0.9810, and 0.9900 (Fig. 10B), respectively. The sensitivities of the GC/SSG-CD-Au electrode for NO_2^- and SO_3^{2-} were 2.7 and 1.5 times higher, respectively, than that for N_2H_4. The SWVs observed at the GC/SSG-CD-Au electrode were highly stable. Additionally, nearly 40% decrease was observed in the sensing ability of the GC/SSG-CD-Au electrode when it was applied to detect the analytes from the mixture. The catalytic activity and sensing ability of the Au NSs at the GC/SSG-CD-Au electrode can be correlated to the larger electrochemically active surface area resulting from the small-sized Au NPs [21].

4. Conclusions

The use of CD as an additive for the sol–gel matrix-modified electrode successfully guided the electrodeposition of small and well-dispersed Au NSs. Such typical Au NSs showed increased active surface area, and the modified electrode was applied for the concurrent electrochemical oxidation and sensing of a mixture of N_2H_4, SO_3^{2-}, and NO_2^-. The concurrent response of the GC/SSG-CD-Au electrode toward the mixture of analytes was demonstrated. The sensitivities of the GC/SSG-CD-Au electrode for the detection of N_2H_4, SO_3^{2-}, and NO_2^- were found to be 0.0310, 0.0490, and 0.0870 μA/μM, respectively. A wide linear range of 100-800 μM, stability, high sensitivity, and well-resolved oxidation peaks were observed for the GC/SSG-CD-Au electrode. The facile fabrication of the GC/SSG-CD-Au electrode may serve as a simple methodology to detect specific compounds in industrial effluents and the aquatic environment. The present research can help to construct electrochemical sensor devices that sense a variety of potentially important molecules.

Acknowledgements

This research was supported by a Post-Doctoral Research Program (2015) of the Incheon National University (INU), Korea.

References

[1] Ismail, A. A., Harraz, F. A., Faisal, M., El-Toni, A. M., Al-Hajry, A., & Al-Assiri, M. S., *Materials and Design,* **2016**, *109*, 530-8.
[2] M.M. Rahman, A. Khan, H.M. Marwani, A.M. Asiri, *Microchimica Acta,* **2016**, *183*(5), 1787-96.
[3] R. Arce, M.J. Aguirre, J. Romero, *ECS Transactions,* **2014**, *64(1),* 37-42.
[4] R. Liu, J. Zhao, Z. Huang, L. Zhang, M. Zou, B. Shi, et al, *Sensors and Actuators, B: Chemical,* **2017**, *240*, 604-12.
[5] S. Garrod, M.E. Bollard, A.W. Nicholls, S.C. Connor, J. Connelly, J.K. Nicholson, et al., *Chemical Research in Toxicology,* **2005**, *18(2),* 115-22.

[6] A. Safavi, A.A. Ensafi, *Analytica Chimica Acta,* **1995**, *300(1-3),* 307-11.
[7] H.Y. Qin, Z.X. Liu, W.X. Yin, J.K. Zhu, Z.P. Li, *Journal of Power Sources,* **2008**, *185(2),* 895-898.
[8] S. Durga, K. Ponmani, S. Kiruthika, B. Muthukumaran, Journal of Electrochemical Science and Technology, **2014**, *5*(*3*), 73-81.
[9] I. Kang, W-s. Shin, S. Manivannan, Y. Seo, K. Kim, Journal of Electrochemical Science and Technology, **2016**, *7*(*4*), 277-285.
[10] E. Dinçkaya, M.K. Sezgintürk, E. Akyilmaz, F.N. Ertaş, *Food Chemistry,* **2007**, *101(4),* 1540-1544.
[11] C.A. Caro, F. Bedioui, J.H. Zagal, *Electrochimica Acta,* **2002,** *47(92),* 1489-1494.
[12] X.H. Pham, C.A. Li, K.N. Han, B.C. Huynh-Nguyen, T.H. Le, E. Ko, et al., *Sensors and Actuators, B: Chemical,* **2014**, *193(2014)*, 815-822.
[13] A.A. Ensafi, M. Amini, *Sensors and Actuators, B: Chemical,* **2010,** *147(1),* 61-66.
[14] M. Shanmugam, K. Kim, *Journal of Electroanalytical Chemistry,* **2016**, *776*, 82-92.
[15] G. Maduraiveeran, R. Ramaraj, *Electrochemistry Communications,* **2007**, *9(8)*, 2051-2055.
[16] S. Manivannan, R. Ramaraj, *Pure and Applied Chemistry,* **2011,** *83(11),* 2041-2053.
[17] S. Paul, *Journal of Electrochemical Science and Technology,* **2016**, *7(2),* 115-131.
[18] A. Wittstock, V. Zielasek, J. Biener, C.M. Friend, M. Bäumer, *Science,* **2010**, *327(5963),* 319-322.
[19] S. Manivannan, R. Ramaraj, *Chemical Engineering Journal,* **2012**, *210*, 195-202.
[20] F. Jia, C. Yu, Z. Ai, L. Zhang, *Chemistry of Materials,* **2007**, *19(15),* 3648-3653.
[21] S. Manivannan, R. Ramaraj, Journal of Nanoparticle Research, **2013**, *15*(*10*), 1978 (1-13).
[22] S. Jayabal, R. Ramaraj, *Electrochimica Acta,* **2013**, *88*, 51-58.
[23] S. Manivannan, R. Ramaraj, *Journal of Chemical Sciences***, 2009**, *121(5),* 735-743.
[24] G. Maduraiveeran, R. Ramaraj, *Journal of Electroanalytical Chemistry***, 2007**, *608(1),* 52-58.
[25] S. Manivannan, K. Kim, *Electroanalysis***, 2016**, *28(7),* 1608-1616.